

Chapter 6

Interpretation of Imaging Data from Spectralis OCT



Atila Bayer

6.1 Introduction

Advances in spectral-domain optical coherence tomography (SD-OCT) have enabled imaging of the optic nerve head (ONH) anatomic features and more accurate evaluation of the retinal nerve fiber layer (RNFL), and the macular region. Structures such as the lamina cribrosa anterior surface topography [1, 2], termination of Bruch's membrane–retinal pigment epithelium complex [3], border tissue of Elschnig [1], and the scleral canal opening [4] can now be visualized. Overlay of optic disc clinical photographs with SD-OCT images has allowed clinicians to identify structures that correspond to common clinical landmarks, such as the clinical disc margin. New metrics such as the Bruch's membrane opening based minimum rim width (BMO-MRW) provide a more accurate measure of the retinal ganglion cell axons at the level of the ONH. This chapter reviews the properties, available scan patterns and tips on interpretation of the Spectralis OCT printouts (Heidelberg Engineering Inc., Heidelberg, Germany). Spectralis OCT uses an 870-nm wavelength super-luminescent diode laser as a light source and is capable of obtaining scans through a pupil size as small as 2.5 mm. The scanning speed of the first generation Spectralis OCT is 40,000 scans/s (85,000 scans/s in Spectralis OCT2). Scan depth is 1.9 mm with axial resolution of 3.87 μm and transverse resolution of 14 μm . Features of Spectralis OCT include automated anatomic positioning system (APS), and APS-linked unique scan patterns including ONH radial & circle scan (ONH-RC), posterior pole horizontal scan (PPoleH), and posterior pole vertical scan (PPoleV) (Fig. 6.1). These scan patterns facilitate analyses of the ONH, RNFL, posterior pole including measurement of individual retinal layers including ganglion cell layer (GCL) thickness.

A. Bayer

Department of Glaucoma, Dönyagöz Eye Hospital, Ankara, Turkey

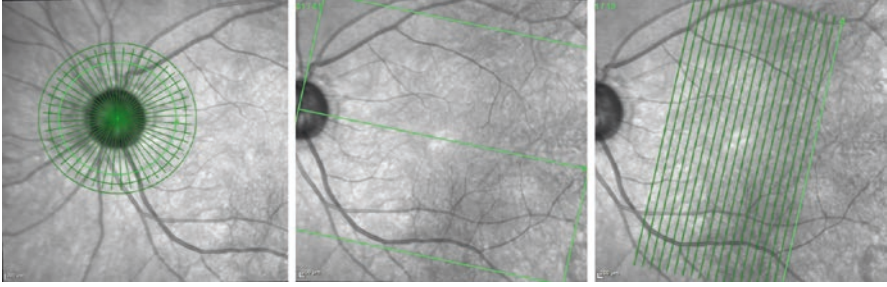


Fig. 6.1 Optic nerve head radial and circle scan (left), posterior pole horizontal scan (center), and posterior pole vertical scan (right) scan patterns of Spectralis optical coherence tomography instrument

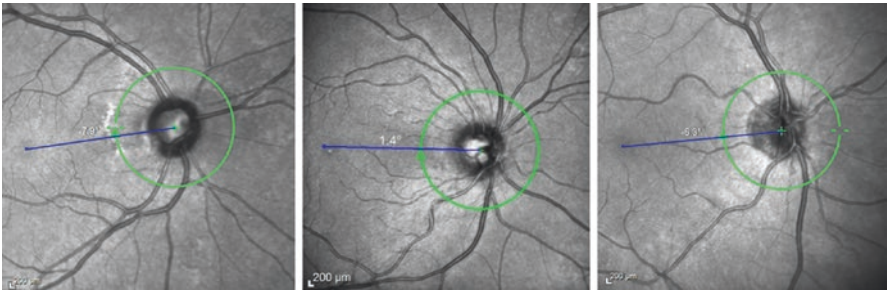


Fig. 6.2 Various examples of the varying angle between the foveal center and the BMO centroid relative to the horizontal axis defined on the fundus image. The mean angle of this axis is about -7° , i.e., the fovea is below the BMO centroid (left image). This angle can be positive (center) where the fovea is above the BMO centroid

6.2 The Automated Anatomic Positioning System

Currently available algorithms of OCT devices report regional data according to temporal, superior, nasal, and inferior sectors, which are established relative to the fixed horizontal and vertical axes of the current image, assuming that neuro-retinal rim width and area in a certain ONH sector refer to approximately the same anatomic location in all human eyes. As seen in clinical fundus images, in most individuals, the fovea is located below the level of the ONH (relative to the horizontal axis of the acquired image frame); the axis connecting the ONH or BMO centroid to foveal center (FoDi or FoBMO axis) deviates from horizontal meridian. A recent study of the angle between the FoBMO axis relative to the horizontal axis defined by the fundus image in 222 white patients with ocular hypertension or glaucoma showed that although the mean angle of this axis was -7° (the fovea being on average 7° below), the range varied from -17° to $+6^\circ$ (Fig. 6.2) [5]. OCT databases that do not correct for the FoBMO alignment have wider confidence intervals. Even a slight head tilt can shift the start/stop point of the TSNIT circle scan, adding

alignment error to normative databases [6]. Test-retest variability is expected to be greater without alignment.

Fovea-to-Disc (FoDi) alignment function of the previous Spectralis OCT algorithm corrected for unwanted eye rotation. Two anatomically fixed landmarks relative to each other, center of the fovea and center of the ONH, define the coordinate system of the eye. FoDi technology ensured all circle scans start/stop at the same anatomical point, providing point-to-point accuracy between consecutive scans and eliminating alignment error in relation to the normative database.

The Glaucoma Module Premium Edition (GMPE) software of Spectralis OCT offers Automated APS which aligns follow-up scans with the baseline image according to FoBMO axis. As mentioned below, BMO is the outer anatomic boundary of the area where axons exit the eye and is used in preference to the FoDi axis. Since the anatomic path of the ganglion cell axon bundles between the fovea and the ONH is organized relative to the FoBMO axis, it is an anatomically consistent landmark for the regionalization of the ONH and retinal tissues [7, 8]. FoBMO alignment, therefore, ensures that all eyes are anatomically aligned correctly with the healthy control eyes (normative database), improving accuracy of measurements (Fig. 6.3). APS-based scan patterns are ONH radial scan for ONH analysis, ONH circle scanning for RNFL analysis, PPoleH scanning for thickness and asymmetry analyses of various retinal layers, and PPoleV for ganglion cell thickness analysis.

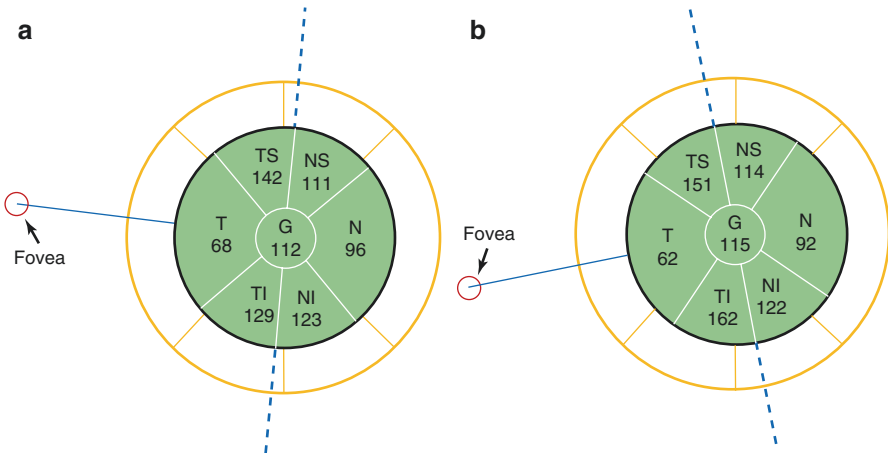


Fig. 6.3 If the correct anatomic orientation is ignored during acquisition of OCT scans, artificially large inter-subject differences in sectorial analyses are likely to occur. Blue line represents the Fovea to Bruch's membrane opening (FoBMO) axis of the individual eye. Two eyes with different anatomical positions of the fovea relative to the Bruch's membrane opening centroid are shown (a and b). Spectralis OCT scan orientation automatically is aligned along the eye's FoBMO axis. If the horizontal and vertical axes of the image frame are fixed (yellow grid), this would result in an orientation shift of the classification sectors relative to the normative database. When optic nerve head anatomy is not aligned with healthy control eyes, normal tissue may appear thin or thin tissue may appear normal leading to significant classification errors

6.3 Scan Properties of Spectralis OCT for Peripapillary Region

6.3.1 Standard 12 Degrees Scan Pattern

The original RNFL imaging algorithm of Spectralis OCT was based on a peripapillary circular scan 12° in diameter (which equates to a retinal diameter of 3.46 mm in eyes with average corneal curvature and axial length). It is automatically centered around the optic disc and 768 data points are analyzed (496 data points on the Z axis, 1.9 mm in depth). The temporal point where the FoDi or FoBMO axis crosses the measurement circle is designated as 0°; degrees are counted in a clockwise direction in the right eye and in counterclockwise direction in the left eye. The device also provides RNFL measurements in sectors consisting of temporal (316°-45°), temporal superior (46°-90°), nasal superior (91°-135°), nasal (136°-225°), nasal inferior (226°-270°), and temporal inferior (271°-315°) sectors. Measurements are compared to the normative database and displayed on the RNFL profile graph as well as quadrant and sectoral pie graphs. Normative database of the standard RNFL analysis (2009) included 218 eyes of healthy European subjects with ages between 20 and 87 years.

6.3.2 The Glaucoma Module Premium Edition

During RNFL analysis with GMPE software, three circle scans of 3.5, 4.1, and 4.7 mm are automatically centered around the BMO centroid and 768 data points are analyzed. The 3.5 mm RNFL circle scan is the default scan for analysis and is comparable to the standard 12° RNFL scan pattern. The two additional wider scans become important when the inner 3.5 mm circle is not interpretable due to confounding pathology such as peripapillary atrophy. In addition to the circular scans, the GMPE software performs 24 radial equidistant scans for ONH analysis (see below) (Fig. 6.4). RNFL thickness analysis is adjusted for BMO area and age on all three scans for a BMO area range of 1.0–3.4 mm². Measurements are compared to the normative database and represented on the RNFL profile graph as well as quadrant and sectoral pie graphs. The current normative database of GMPE (2014) includes 246 eyes of healthy European subjects aged between 20 and 87 years.

6.4 Features of the Glaucoma Module Premium Edition Software for the Optic Nerve Head

6.4.1 The Optic Disc Margin

The optic disc margin or clinical disc margin is a clinical construct for the boundary that surrounds the neural tissue within the ONH. All quantitative measurements of the neuro-retinal rim with modern imaging techniques require the identification of

OD. IR 30° ART + OCT 15.0° (4.4 mm) ART (23) Q: 34 [HR]

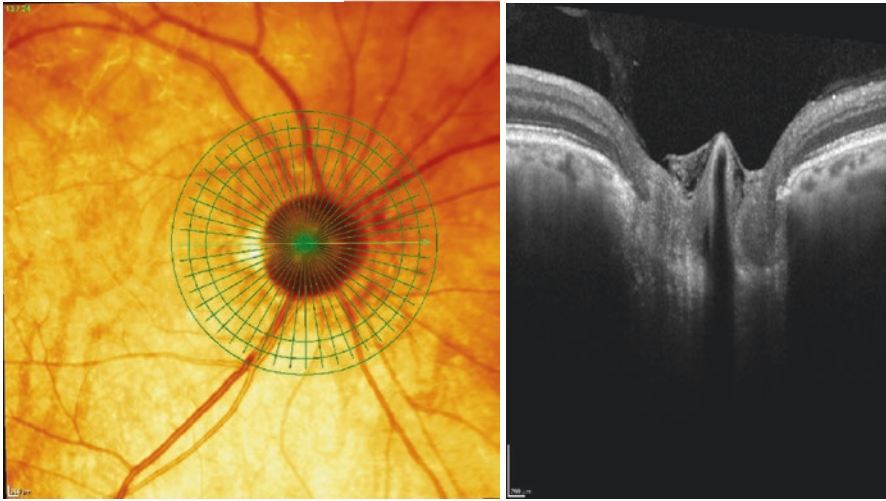


Fig. 6.4 The Glaucoma Module Premium Edition software provides three circle scans (3.5, 4.1, 4.7 mm) for measuring the retinal nerve fiber layer and 24 radial scans for measurement of the Bruch's membrane opening-minimum rim width. The tomogram on the right shows the optic nerve head B-scan through the plane shown as an arrow on the fundus image

the disc margin. Traditionally, optic disc margin has been defined as the inner edge of the scleral rim and has been assumed to be a single and consistent anatomic structure around the ONH. Optic disc margin has been considered the true outer border of the neuro-retinal rim from which the width of the rim could be measured. However, what the clinician identifies as the disc margin in an individual eye is rarely a single structure. SD-OCT analysis of the ONH structures has revealed that the structures creating the appearance of the clinical disc margin vary according to configuration and relationship of the peripapillary tissues including the border tissue of Elschnig, sclera, and choroid and is highly variable within and between individual eyes. Histologic findings in monkey eyes and SD-OCT findings in human eyes have revealed that the clinical optic disc margin is rarely a single anatomic entity, nor are the structures that underlie it consistent in an individual eye [3, 9]. The structure corresponding to the optic disc margin at the 3 o'clock position may be different to that at the 9 o'clock position.

6.4.2 *Bruch's Membrane Opening*

The termination of Bruch's membrane around the ONH is defined as the BMO, which represents the opening through which all axons exit the eye. Axons cannot cross Bruch's membrane and must exit the eye beyond its edge [10]. The BMO defines the outermost edge of neural tissue at the level of the disc. While the BMO is consistently detected by SD-OCT imaging, it is rarely clinically visible in humans. The Bruch's membrane can extend beyond Elschnig border tissue (BT) or

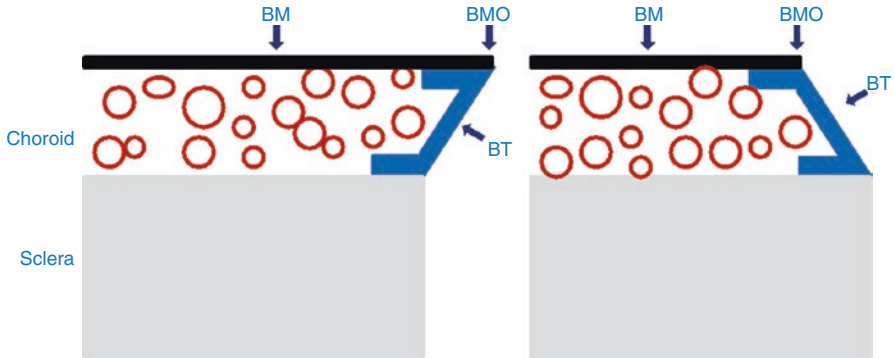
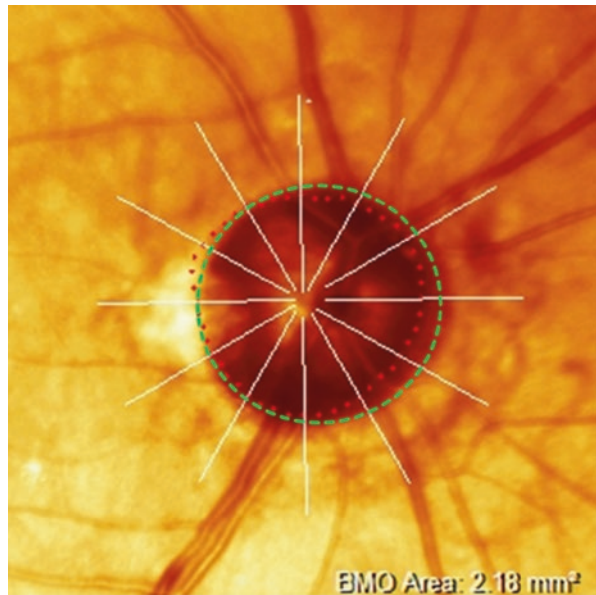


Fig. 6.5 Bruch's membrane configuration relative to the border tissue of Elschnig (BT). The BT configuration may be internally (left) or externally oblique (right). *BM* Bruch's membrane, *BMO* Bruch's membrane opening, *BT* Border tissue of Elschnig [3]

Fig. 6.6 Pseudo-color fundus image of a glaucoma patient demonstrates Bruch's membrane opening demarcation (red dots) based on automated segmentation by Spectralis OCT. Clinical disc margin is demarcated by green dashed curve. Note that the two do not overlap in most parts of the circumference of the optic nerve head



vice-versa (Fig. 6.5) creating various configurations around the ONH (Fig. 6.6) [3, 11].

The GMPE software automatically detects 48 BMO positions along 24 equidistant scan lines centered on the ONH centroid to determine the BMO-based disc margin (Figs. 6.1 and 6.4). BMO is a useful landmark in glaucoma given its relative stability under a variety of conditions. The BMO remains unaltered despite large changes in intraocular pressure caused by glaucoma surgery [12].

Corneal curvature (CC) is an important factor to account for in order to obtain accurate measurements. The RNFL is thicker closer to the disc margin and thins out

with increasing distance from the BMO. Therefore, the RNFL circle scan should be consistently placed for accurate assessment and comparison of RNFL measurements relative to the normative database. In an eye with flat cornea, the measurement circle falls closer to the BMO centroid and should be displaced away from the BMO centroid and vice versa. Therefore, before image acquisition, it is recommended to change the standard 7.7 mm corneal curvature value and enter the individual eye's mean corneal curvature. With the help of this CC value and the specific focus setting, the software is able to correct for image magnification or minification. Therefore, exact, diameters of the circle scans can be guaranteed.

6.4.3 The Neuro-Retinal Rim

The most anterior part of ONH contains the RGC axons, which make up the neuro-retinal rim. Figure 6.7 shows a B-scan displaying the structures of the ONH from the internal limiting membrane to the anterior lamina cribrosa. The neuro-retinal rim is separated from the vitreous by the inner limiting membrane (ILM) of Elschnig. ILM is an objective inner boundary of neuro-retinal rim tissue that is consistently

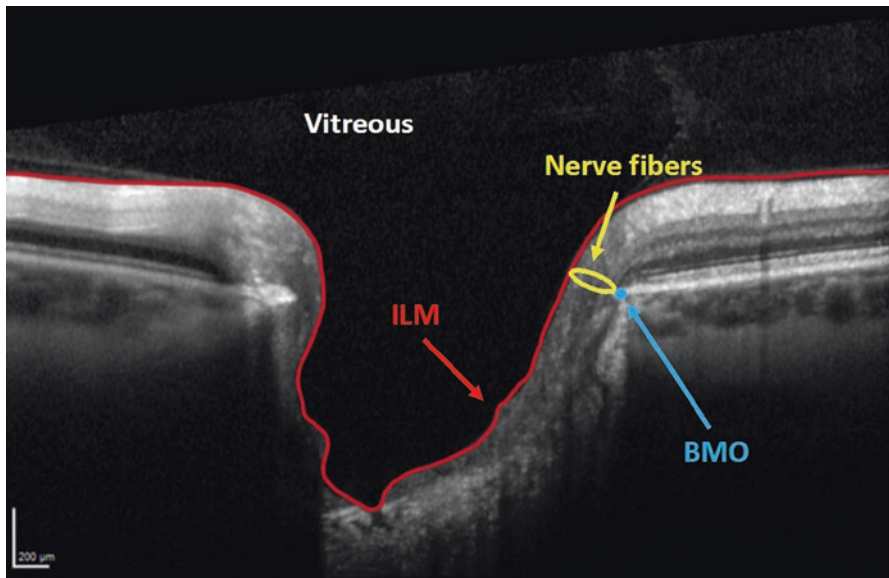


Fig. 6.7 The most anterior part of the optic nerve head contains the retinal ganglion cell axons, which make up the neuro-retinal rim. The neuro-retinal rim is separated from the vitreous by the internal limiting membrane. The Bruch's membrane opening represents the outer border of the rim tissue (nerve fibers), which is represented as a yellow ring. *BMO* Bruch's membrane opening, *ILM* internal limiting membrane

detected by SD-OCT. In order to avoid overestimation or underestimation, rim tissue must be measured in the correct geometric orientation. Ganglion cell axons may exit the eye almost parallel to the visual axis or even perpendicular to it. Significant errors in rim measurements can occur if the measurement plane is fixed.

Because of the varying orientation of the RGC axons upon their entry into the neural canal relative to the BMO, Povazay et al. and Chen and collaborators proposed that the minimum distance from BMO-RPE complex to the ILM represents the most accurate measurement of the axonal content in the neuro-retinal rim [13, 14]. The BMO is currently used as a reference by Spectralis OCT and the rim width is quantified as the minimum distance between the BMO and the internal limiting membrane. Chauhan and Burgoyne subsequently suggested using the end of the Bruch's membrane proper for this purpose and explored the difference between this measurement, termed BMO-minimum rim width (BMO-MRW) and conventional measurements, called horizontal rim width (BMO-HRW), and demonstrated the superiority of the BMO-MRW measurements (Fig. 6.8) [11, 15]. Strouthidis and associates showed the utility of BMO-MRW for detection of progressive ONH change in experimental primate glaucoma [9].

As mentioned above, the BMO-MRW analysis uses 48 equidistant data points, at which the BMO is identified and BMO-MRW calculated using an automated segmentation algorithm. The "BMO Overview" tab shows an overview of ONH anatomy at 12 equidistant locations around disc margin (Fig. 6.9) [16]. Clock hour anatomy is provided to the clinician for confirmation of automated segmentation, in addition to quantification of BMO-MRW to enhance clinical disc examination. Comparison to the normative database is then performed and results displayed as color-coded arrows. The neuro-retinal rim tissue is assessed perpendicular to the orientation of the axons and therefore, the varying trajectory of nerve fibers entering the ONH is taken into account at all points of measurement.

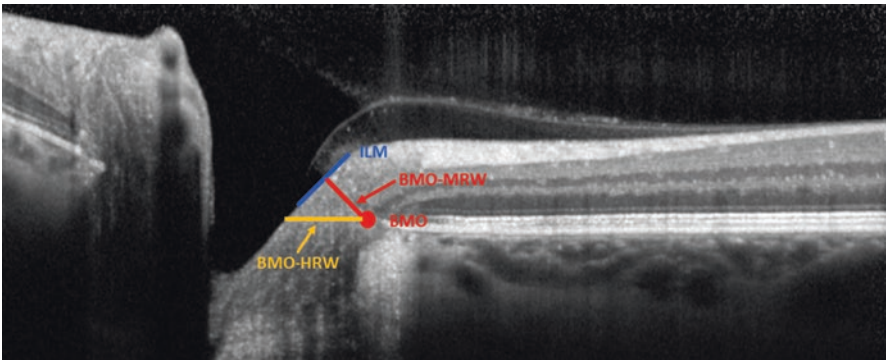


Fig. 6.8 The minimum distance from the Bruch's membrane opening to the internal limiting membrane represents the most accurate measurement of the neuro-retinal rim width. *BMO* Bruch's membrane opening, *BMO-MRW* Bruch's membrane opening-minimum rim width, *BMO-HRW* Bruch's membrane horizontal rim width, *ILM* internal limiting membrane

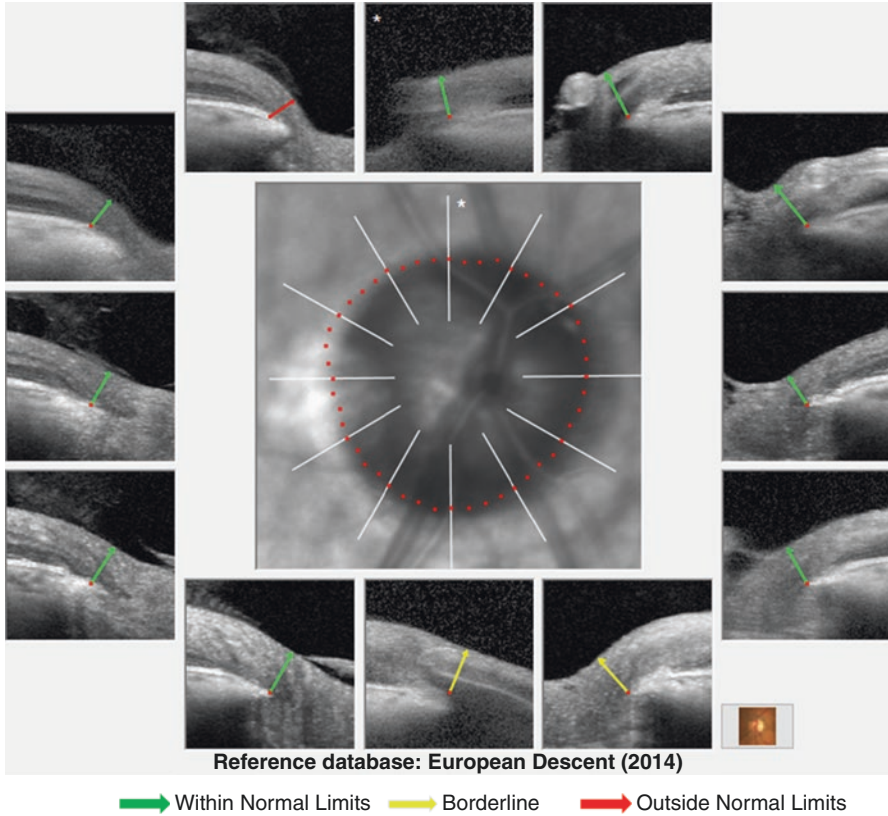


Fig. 6.9 Overview of the Bruch's membrane opening-minimum rim width (BMO-MRW) report of a patient with glaucomatous damage in the right eye. In the infrared image, the red dots represent Bruch's membrane opening delineated by the automated segmentation algorithm of Spectralis OCT at 48 equidistant points. The anatomic basis for BMO-MRW calculation at 12 equidistant locations around disc margin are also provided; classification of each location relative to a normative database is shown by color-coded arrows

The BMO segmentation should be confirmed after acquiring the ONH-RC scan. The BMO can sometimes be hidden by anatomical structures such as an overlying vessel; other times, it cannot be distinguished from neighboring structures due to the similar reflectivity. In such cases, changing the contrast scale from the standard settings of 12 to for example 15 may allow better visibility of the ONH structures. Detecting the wedge-shaped ending of the choroid may also be helpful in finding the BMO. It is well known that choriocapillaris does not exist without Bruch's membrane. Therefore, the BMO never ends before the choriocapillaris does, but it can extend further towards the ONH. The arrow representing the BMO-MRW should not cross retinal layers other than RNFL. There may be a jag in the height profile. This might indicate outlying BMO points or a wrong ILM segmentation.

In such a case, the segmentation of the OCT scan can be checked by placing the blue vertical lines onto the peak in the height profile. When it is not possible to detect the BMO point in one OCT scan, it is better to scroll through the neighboring scans till one BMO point has been identified clearly. After this, scan line should be dragged and dropped to the identified BMO point.

The BMO area affects the BMO-MRW profile. According to the ISNT rule, the thickness profile should show a slight double hump. In eyes with a small BMO area, the thickness profile graph is shifted upward (thicker) and for large BMO area, the thickness profile graph is shifted downward (thinner). Individual BMO-MRW height profile should be compared (black) with the BMO area- and age-adjusted normative database (green). Notches occur in case of rim thinning commonly matching RNFL defects. Since averaging can hide focal axonal defects in the classification chart, it is strongly recommended to review the height profile meticulously. The inferior and superior regions of the height profile should not be located below the nasal height profile; otherwise, the ISNT rule is clearly not respected.

6.5 The Posterior Pole Horizontal Algorithm (PPoleH)

The PPoleH scan is a volume scan of a $30^\circ \times 25^\circ$ area centered on the fovea. It consists of 61 horizontal B-scans aligned with the individual eye's FoBMO axis. The volume scan includes the total retinal thickness from the macula to the ONH across the posterior pole so that the complete path of the RGC axonal complex from the origin up to the entry point into the ONH can be assessed for macular RGCs (Fig. 6.10). Automated segmentation of the individual layers by the GMPE software allows evaluation of the thickness maps of the layers of interest in glaucoma (RNFL, GCL or IPL). The PPoleH scan covers the macular area corresponding to the majority of locations on the 24-2 visual field test for better structure and function correlation. The color scale of the posterior pole thickness map is finer than the standard retina thickness map and therefore, it is more sensitive for visualization of glaucomatous changes.

6.5.1 The Posterior Pole Asymmetry Analysis

The posterior pole asymmetry analysis is carried out by the software after a PPoleH scan. In the posterior pole asymmetry analysis tab, the posterior pole thickness map, the OCT raw scan for checking layer segmentation, and the posterior pole hemisphere asymmetry analysis are included.

The Posterior Pole Asymmetry Analysis combines mapping of the posterior pole retinal thickness with asymmetry analysis between the two eyes of the same individual and between the superior and inferior hemispheres of the same eye. Only the central $24^\circ \times 24^\circ$ of the macular volume scan is segmented and an 8×8 grid displaying retinal thickness on 3° superpixels is provided. Between-eye and superior-inferior thickness differences are also shown as a grayscale map where

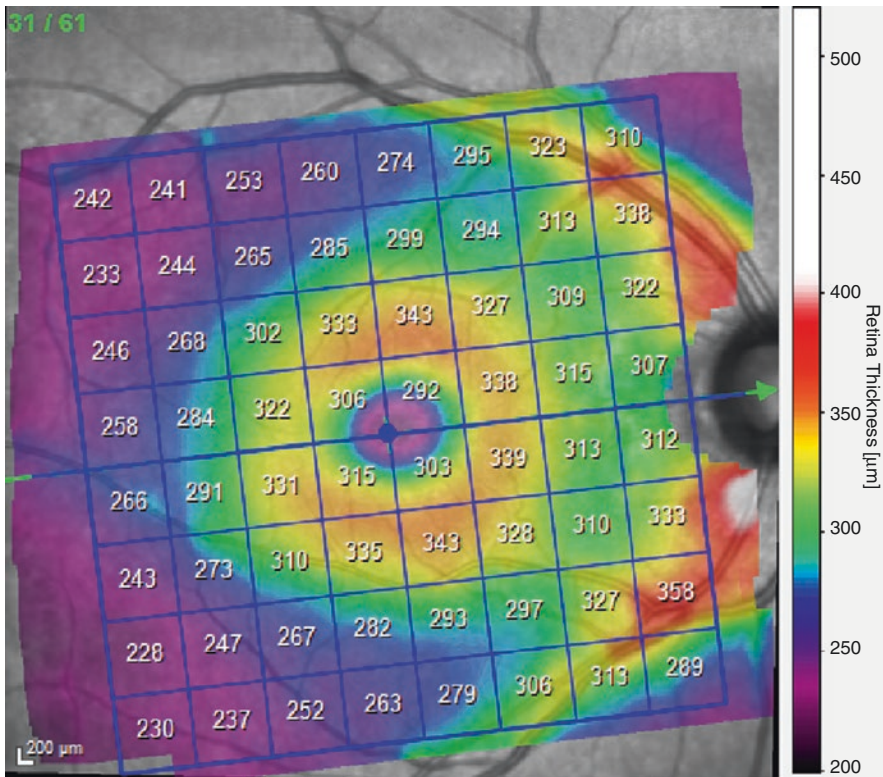


Fig. 6.10 Posterior pole horizontal scan of a healthy subject. The warmer colors on the thickness map represent thicker retina. The prominent thicker arcuate temporal-inferior and temporal-superior nerve fiber bundles appear red. The fovea as well as the peripheral retina appear purple or blue caused by physiologically thinner values

darker colors represent retinal thinning compared to the corresponding superpixel in either the fellow eye or the fellow vertical hemisphere. A difference of $30\ \mu\text{m}$ results in a black superpixel indicating a significant difference. Three dark squares next to each other can indicate a defect (Fig. 6.11). Thickness differences along the nasal most superpixels are commonly caused by physiologically asymmetric distribution of the arteries and veins.

6.6 Posterior Pole Vertical Scan (PPoleV)

Pathologies of the outer retinal layers may affect the posterior pole thickness map. The PPoleV algorithm is an alternative macular volume scan. Nineteen vertical B-scans, encompassing a $30^\circ \times 15^\circ$ scanning area, are carried out perpendicular to the FoBMO axis. These high resolution and noise-reduced scans allow for clear visualization of GCL and IPL layers after segmentation. Vertical scans provide more

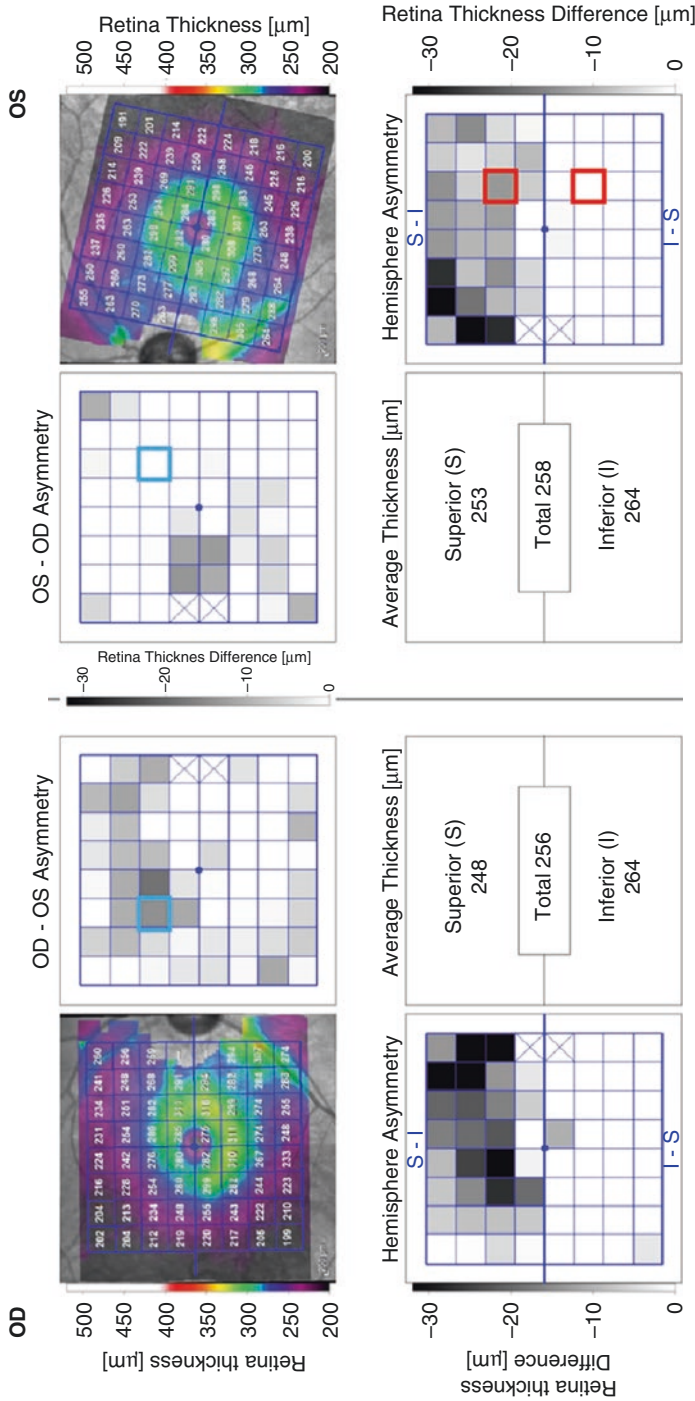


Fig. 6.11 Bilateral posterior pole asymmetry analysis of a patient with glaucoma. There is damage in both the superior and inferior nerve fibers in both eyes. This can be seen in the retinal thickness maps as thinning of the arcuate fibers both superiorly and inferiorly, and is more prominent superiorly in both eyes. In the hemisphere asymmetry charts, most of the squares in the superior hemisphere has colors with various tones of gray, representing thinning of the retina compared to the corresponding squares in the inferior hemisphere in both eyes. As an example, the red surrounded square in the upper hemisphere of the left eye shows a thickness of 269 microns, which is 14 microns thinner than the red surrounded corresponding square in the lower hemisphere. In the OD-OS asymmetry chart the blue surrounded square in the right eye shows a thickness of 254 microns, which is 15 microns thinner than the corresponding location in the left eye. This square has a gray color, representing thinning of the retina compared to the white colored corresponding square in the left eye.

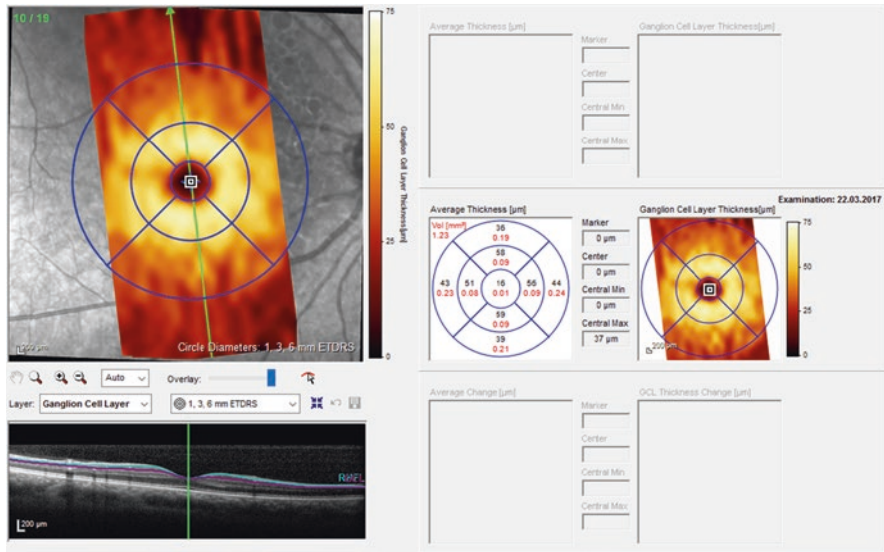


Fig. 6.12 Heat map of the ganglion cell layer of a healthy eye obtained following posterior pole vertical analysis and segmentation. Average thickness and volume measurements are provided on an ETDRS grid

sensitive symmetry analysis of superior vs. inferior macular layers on each individual B-scan and major horizontal vasculature does not create shadowing. Specifically, the GCL thickness is symmetrical between the superior and inferior macular hemispheres compared to the temporal and nasal hemispheres; The vertical asymmetry in GCL across the horizontal meridian was reported to be the most sensitive biomarker for detection of various stages of glaucoma including the preperimetric stage [17, 18].

After the PPoleV analysis and manual or automated segmentation, GCL thickness is provided as a color map on a circular grid. This thickness map can be displayed as a standard heat map (Glow Scale) (Fig. 6.12) or color map (Color Scale). Lack of a continuum of colors in the color map may lead to misleading of thickness values as some borderline values may fall in one color spectrum vs. another. Since heat maps offer a more continuous spectrum of color-scales, the standard heat map is preferred. Ganglion cell layer thickness maps and average thickness values are provided in a ETDRS grid format.

6.7 Interpretation of the Printouts

6.7.1 The Standard RNFL Single Exam Report

See Fig. 6.13.

- 1. Patient and Test Information:** Displays general patient information including patient name, patient ID, diagnosis, date of birth, examination date and gender.

RNFL Single Exam Report OU
SPECTRALIS® Tracking Laser Tomography



Patient:
Patient ID:
Diagnosis: ---

1

DOB:
Exam.: 23.Mar.2017
Comment: ---

Sex: F

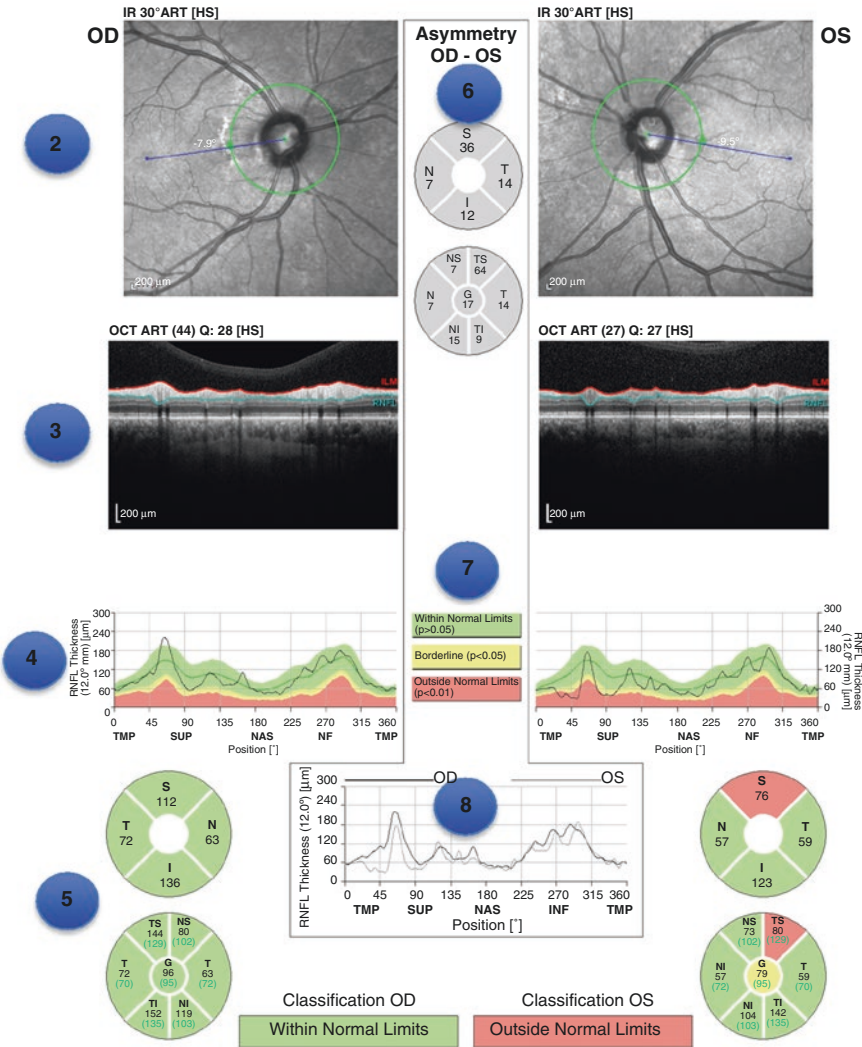


Fig. 6.13 The standard RNFL single exam report of a patient with a glaucomatous superior RNFL defect in the left eye. This eye is classified as outside normal limits. The right eye is classified as within normal limits

The examiner should verify the name and date of birth of the patient, as the results are compared to age-matched data from the normative database.

2. **Fundus Image Information:** The infrared reflectance (IR) image is an image of the fundus where the peripapillary circular scan is delineated. This image should be checked for even illumination, as well as proper location of circular scan, and fovea to disc alignment (or FoDi) axis. Abnormalities such as myelinated nerve fibers, peripapillary atrophy, and vitreous opacities should be excluded. The string above each fundus image notes the settings used for that image. In this example:

- (a) “IR” is imaging modality.
- (b) “30°” is the field of view.
- (c) “ART” indicates that the automatic real-time function was active during image capture.
- (d) “[HR]” is the resolution setting (High Speed/High Resolution).

3. **RNFL Profile Image:** RNFL profile (raw image) should be checked for abnormalities of the vitreo-retinal interface as well as the segmentation errors.

The string above each OCT image notes the settings used for that image. In this example:

- (a) “ART” indicates that the automatic real-time function was active during image capture.
- (b) “(44)” is the number of averaged frames, i.e., the number of times the circular scan was repeated.
- (c) “Q:28” is the Quality score on a scale of 1–40. Values of <20 are considered poor quality image.
- (d) “[HR]” is the resolution setting (High Speed/High Resolution).

4. **RNFL Thickness Profile:** The black line indicates the thickness values of the patient’s scan around the optic disc starting from 9 o’clock in the temporal quadrant (3 o’clock in the left eye) and going through the superior, nasal, inferior quadrants to end in the temporal quadrant (TSNIT). Background colors indicate normative data ranges (see Classification Colors). The dark green line plots the average thickness values from the normative database. Thickness profile should be characterized by distinctive humps along the temporal superior and temporal inferior sectors and values should fall within the range of normal limits for all sectors.

5. **Classification Chart:** The RNFL thickness is averaged and compared to the normative database in four quadrants and six sectors (temporal, temporal superior, nasal superior, nasal, nasal inferior, temporal inferior), as well as globally. This chart shows the average RNFL thickness (in microns) for each sector of each eye. Global (G) average is shown in the center. Sector colors indicate classification compared to the normative database. The black numbers represent the

average RNFL thickness in each sector. The numbers in parentheses (green) are the expected normal values, adjusted for age. The classification bar displays the classification of the worst sector in the pie graph.

6. **The Asymmetry Chart:** Displays the difference (in microns) between the thickness of corresponding quadrants (top) or sectors (bottom) of the right and left eye. If the RNFL thickness is similar in the two eyes, the value will be close to zero.
7. **Classification Colors:** Indicate comparison against the normative database. Green color represents “Within Normal Limits” values, i.e., measurements within the 95% prediction limits for normality ($p > 0.05$). Yellow represents “Borderline”, with values outside the 95% but within 99% prediction interval of the normal distribution ($0.01 < p < 0.05$). Red color represents “Outside Normal Limits”, with RNFL thickness measurements less than 99% of the healthy population ($p < 0.01$).
8. **Combined RNFL Profile:** Provides plots the RNFL thickness graph of both eyes. If the correlation between the two eyes is good, the lines on the graph will be very similar.

6.7.2 *The RNFL Single Exam Report of the Glaucoma Module Premium Edition Software*

GMPE’s RNFL single exam report is similar to the standard report with a few differences. As mentioned above, the GMPE software performs three circle scans (3.5, 4.1, 4.7 mm in diameter). All scans are aligned with the individual eye’s FoBMO axis. Since the normative database is different than the standard report and takes the BMO area into consideration, the classification chart has some differences from the standard report that are summarized below (Fig. 6.14).

1. **Fundus Image Information:** Interpretation of the IR fundus image is similar to that of standard report. In the GMPE report, although the default setting of circular scan is 3.5 mm, it is possible to see the results of the other two circular scans 4.1 and 4.7 mm in diameter. The setting of the current circular scan is shown in bold. The circle scan diameter and BMO area is presented in the right lower section of the fundus image.
2. **Classification Chart:** RNFL thickness is analyzed and classified in four quadrants, Garway-Heath sectors and globally. The two charts show average RNFL thickness (in microns) for each sector and quadrant. Global (G) average is shown in the center of the former. Sector or quadrant color indicates classification based on the normative database of the GMPE. The black numbers represent the average RNFL thickness values in each sector. The numbers in parentheses shows the ranking of the RNFL thickness in percentile within the normative database.

RNFL Single Exam Report OU
SPECTRALIS® Tracking Laser Tomography



Patient: Patient ID: 1 Diagnosis: --- DOB: Exam.: 23.Mar.2017 Comment: --- Sex: F

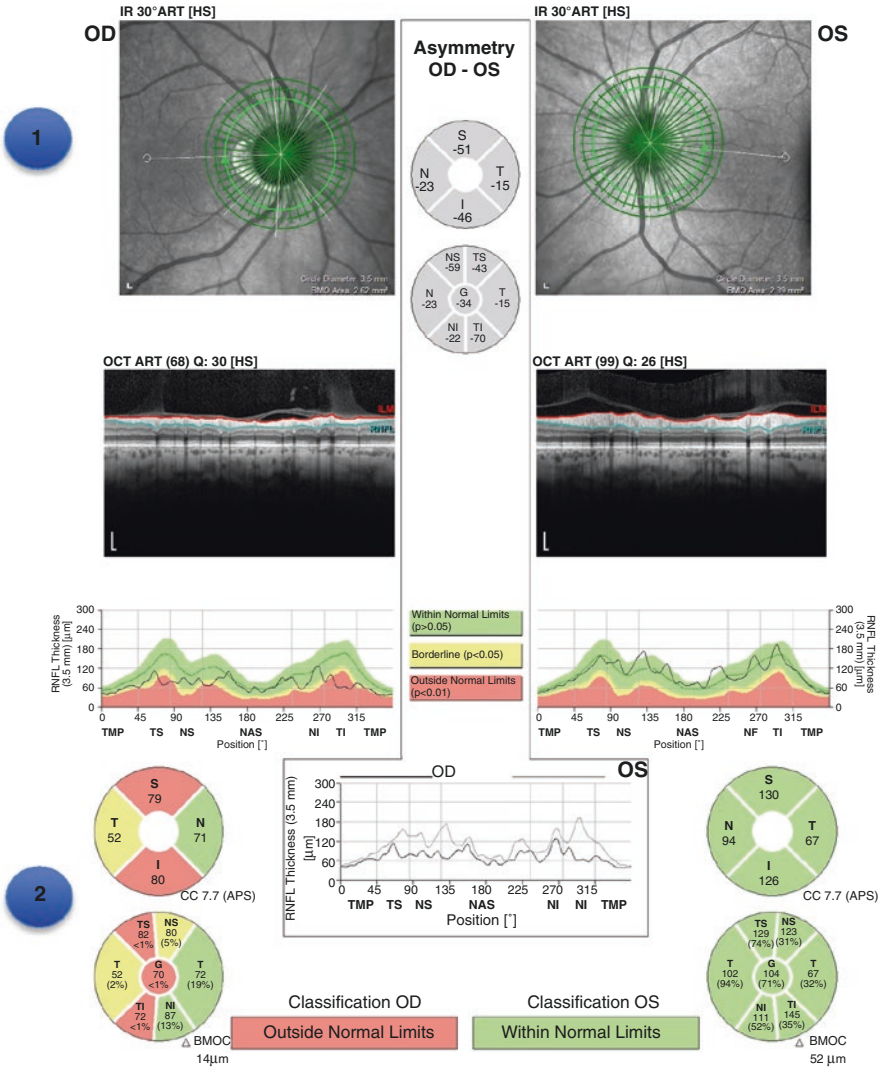


Fig. 6.14 Glaucoma Module Premium Edition software RNFL single exam report of a patient with glaucomatous superior, temporal and inferior RNFL defects in the right eye on the 3.5 mm circle scan. This eye is classified as outside normal limits. The left eye is classified to be within normal limits

Classification colors are similar to that of the standard RNFL report. The classification bar in the bottom displays the classification of the worst sector in the pie graph. CC represents corneal curvature, and Δ BMO shows the distance between the BMO and the optic disc centroids.

6.7.3 The Minimum Rim Width Analysis Report of the Glaucoma Module Premium Edition Software

See Fig. 6.15.

1. **Patient and Test Information:** Displays general patient information such as patient name, patient ID, diagnosis, date of birth, examination date and gender. The name and date of birth of the patient need to be verified as the results are compared to age-matched data from the normative database.
2. **BMO Overview Tab:** Shows an overview of ONH anatomy at 12 equidistant locations around the BMO. The BMO area is displayed on the bottom left of the central IR image (1.96 mm² in the right eye and 1.98 mm² in the left eye) and the BMO is marked in red. Arrows show the anatomic structures that form the basis for measurement of the MRW at each location. The color of the arrows flags the classification of the MRW based on the normative database. ILM is represented in red.

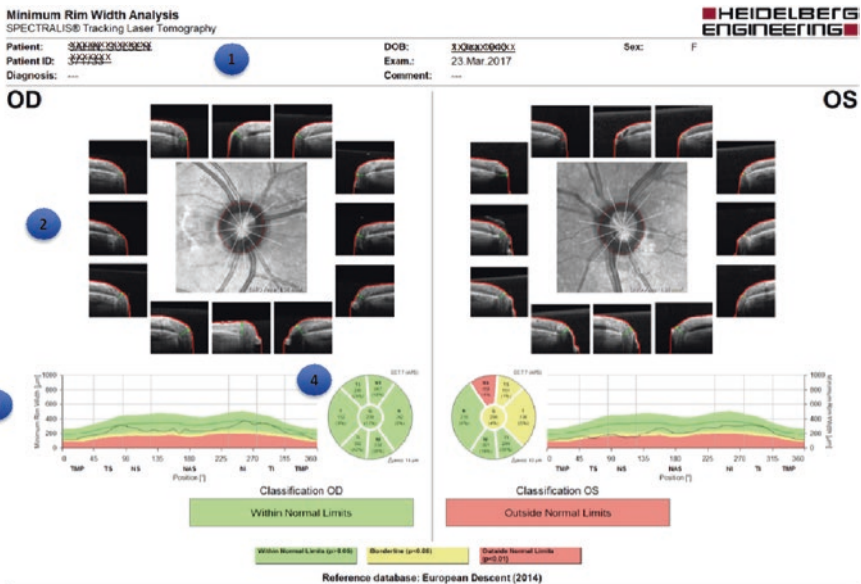


Fig. 6.15 Glaucoma Module Premium Edition software minimum rim width analysis report of the patient in Fig. 6.13 with superior and temporal glaucomatous rim thinning in the left eye. This eye is classified as outside normal limits. Right eye is classified as within normal limits

3. **BMO-MRW Height Profile (TSNT Graph):** The measured BMO-MRW is provided in color codes and in microns along the optic disc circumference starting from 0° , which is the point located temporally at the junction of the FoBMO axis and BMO. The black curve indicates the thickness values of the patient's scan. Age and BMO area adjusted MRW of normal eyes is also represented in the height profile as a green curve. The height profile should show a slight double hump according to the ISNT rule. In a case with glaucoma, the MRW profile does not show a temporal inferior and temporal superior hump and the ISNT rule is not fulfilled. Notches in the temporal inferior or temporal superior height profile correspond to focal neuroretinal rim loss or nerve fiber bundle defects.
4. **Classification Chart:** The measured average BMO-MRW thickness in microns, corresponding percentiles of the normal distribution adjusted for age and the BMO area of the individual eye are shown for each individual Garway-Heath sector (T, TS, NS, N, NI, TI) and globally. The black numbers represent the average MRW thickness values in each sector. The numbers in parentheses shows the percentile of the MRW thickness value of that sector. Classification colors are similar to that of the standard RNFL report. The overall classification bar below the Garway-Heath sector map reflects results of the thinnest sector. Classification colors are similar to the previous reports. CC represents corneal curvature, and Δ BMO shows the distance between the BMO and the optic disc centroids.

6.7.4 *The Posterior Pole Asymmetry Analysis Report*

See Fig. 6.16.

1. **Patient and Test Information:** Displays general patient information as patient name, patient ID, diagnosis, date of birth, examination date and gender.
2. **Posterior Pole Thickness Map:** In each $3^\circ \times 3^\circ$ superpixel on the 8×8 grid, the average retinal thickness within the superpixel is displayed. The warmer (the redder) the color of the thickness map, the thicker the measured retinal area. The compressed color scale on the right side of the map is used to localize even the smallest differences in retinal thickness between adjacent areas.
3. **Inter-Ocular Asymmetry Map:** The retinal thickness at 64 superpixels in one eye is compared to the corresponding thickness measurements in the fellow eye. Superpixels with shades of gray demonstrate reduced thickness compared to the corresponding superpixels in the fellow eye. The intensity of the gray scale reflects the magnitude of differences between corresponding superpixels of the eyes.
4. **Hemisphere Asymmetry Map:** The average retinal thickness in superpixels in one hemisphere is compared to the corresponding superpixels in the opposite hemisphere. Superpixels displaying various shades of gray in one hemisphere have reduced thickness compared to those on the corresponding hemisphere. The intensity of the gray color is a function of the amount of difference between corresponding superpixels of the two hemispheres (black: $\geq 30 \mu\text{m}$ difference).

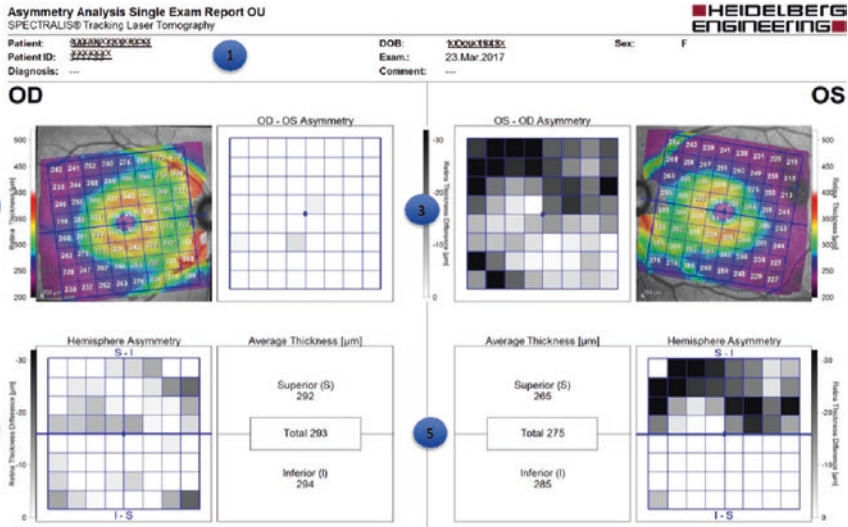


Fig. 6.16 The Posterior Pole Asymmetry analysis of the patient in Figs. 6.13 and 6.15. The prominent arcuate temporal-inferior and temporal-superior nerve fiber bundles appear red in the right eye. In the left eye, there is glaucomatous damage in the superior quadrant, which can be seen in the retinal thickness map as thinning of the arcuate fibers superiorly. In the hemisphere asymmetry chart of the left eye, most of the superpixels in the superior hemisphere are flagged various shades of gray, representing thinning of the retina compared to the corresponding superpixels in the inferior hemifield. In the OS-OD asymmetry chart (3), most of the superpixels are flagged with various shades of gray, depicting retinal thinning in the left eye compared to the right eye

5. Average Thickness Chart: The averaged retinal thickness of the central 24° × 24° area is provided in addition to the superior and inferior hemisphere thickness measurements.

6.8 Key Points

- Poor signal strength leads to a faint image resulting in the software being unable to accurately identify the boundaries of the retinal layers. The technician needs to ensure that the patient blinks just before image acquisition or instill artificial tears to improve the image quality.
- The eye typically has five micro-saccades per second. Unless there is image tracking, motion artifact is very likely even with the most cooperative patient. That is why a decrease in image acquisition time improves image quality.
- Accurate acquisition of the image without cutoff at the edges and with good centration of the optic nerve or the fovea is very important for an acceptable test.
- After confirming that all the requirements have been met, the physician must rule out the presence of coexisting pathology that may confound the results and therefore, the interpretation. The most common offenders include vitreous

traction on the RNFL and epiretinal membranes in the peripapillary and macular region.

- The physician should confirm that the auto-segmentation function of the software has correctly identified the layers it is trying to measure.
- The clinician needs to determine if the patient's ocular condition merits comparison to a normative database. For example, high myopes are not included in OCT normative databases, and therefore, their measurements typically read as abnormal.
- It is very important for the clinician to have ready access to the raw images acquired before looking at the interpretation provided in the report.

References

1. Strouthidis NG, Grimm J, Williams GA, Cull GA, Wilson DJ, Burgoyne CF. A comparison of optic nerve head morphology viewed by spectral domain optical coherence tomography and by serial histology. *Invest Ophthalmol Vis Sci.* 2010;51:1464–74.
2. Lee EJ, Kim TW, Weinreb RN, Park KH, Kim SH, Kim DM. Visualization of the lamina cribrosa using enhanced depth imaging spectral-domain optical coherence tomography. *Am J Ophthalmol.* 2011;152:87–95e81.
3. Reis AS, Sharpe GP, Yang H, Nicoleta MT, Burgoyne CF, Chauhan BC. Optic disc margin anatomy in patients with glaucoma and normal controls with spectral domain optical coherence tomography. *Ophthalmology.* 2012a;119:738–47.
4. Strouthidis NG, Yang H, Reynaud JF, Grimm JL, Gardiner SK, Fortune B, Burgoyne CF. Comparison of clinical and spectral domain optical coherence tomography optic disc margin anatomy. *Invest Ophthalmol Vis Sci.* 2009;50:4709–18.
5. He L, Ren R, Yang H, Hardin C, Reyes L, Reynaud J, Gardiner SK, Fortune B, Demirel S, Burgoyne CF. Anatomic vs acquired image frame discordance in spectral domain optical coherence tomography minimum rim measurements. *PLoS One.* 2014;9:e92225. [PubMed: [24643069](https://pubmed.ncbi.nlm.nih.gov/24643069/)]
6. Valverde-Megías A, Martínez-de-la-Casa JM, Serrador-García M, Larrosa JM, García-Feijóo J. Clinical relevance of foveal location on retinal nerve fiber layer thickness using the new FoDi software in spectralis optical coherence tomography. *Invest Ophthalmol Vis Sci.* 2013;54:5771–6.
7. Jansonius NM, Nevalainen J, Selig B, Zangwill LM, Sample PA, et al. A mathematical description of nerve fiber bundle trajectories and their variability in the human retina. *Vis Res.* 2009;49:2157–63.
8. Hood DC, Raza AS, de Moraes CG, Liebmann JM, Ritch R. Glaucomatous damage of the macula. *Prog Retin Eye Res.* 2013;32:1–21.
9. Strouthidis NG, Fortune B, Yang H, Sigal IA, Burgoyne CF. Longitudinal change detected by spectral domain optical coherence tomography in the optic nerve head and peripapillary retina in experimental glaucoma. *Invest Ophthalmol Vis Sci.* 2011;52:1206–19.
10. Chauhan BC, Burgoyne FC. From clinical examination of the optic disc to clinical assessment of the optic nerve head: a paradigm change. *Am J Ophthalmol.* 2013;156:218–27.
11. Reis AS, O'Leary N, Yang H, Sharpe GP, Nicoleta MT, Burgoyne CF, Chauhan BC. Influence of clinically invisible, but optical coherence tomography detected, optic disc margin anatomy on neuroretinal rim evaluation. *Invest Ophthalmol Vis Sci.* 2012b;53:1852–60.
12. Reis AS, O'Leary N, Stanfield MJ, Shuba LM, Nicoleta MT, Chauhan BC. Lamellar displacement and prelaminar tissue thickness change after glaucoma surgery imaged with optical coherence tomography. *Invest Ophthalmol Vis Sci.* 2012d;53:5819–26.

13. Chen TC. Spectral domain optical coherence tomography in glaucoma: qualitative and quantitative analysis of the optic nerve head and retinal nerve fiber layer (an AOS thesis). *Trans Am Ophthalmol Soc.* 2009;107:254–81.
14. Povazay B, Hofer B, Hermann B, et al. Minimum distance mapping using three-dimensional optical coherence tomography for glaucoma diagnosis. *J Biomed Opt.* 2007;12:041204.
15. Chauhan BC, O'Leary N, Almobarak FA, Reis AS, Yang H, Sharpe GP, Hutchinson DM, Nicoleta MT, Burgoyne CF. Enhanced detection of open-angle glaucoma with an anatomically accurate optical coherence tomography-derived neuroretinal rim parameter. *Ophthalmology.* 2013;120:535–43.
16. Danthurebandara VM, Sharpe GP, Hutchinson DM, Dennis J, Nicoleta MT, McKendrick AM, Turpin A, Chauhan BC. Enhanced structure-function relationship in glaucoma with an anatomically and geometrically accurate neuroretinal rim measurement. *Invest Ophthalmol Vis Sci.* 2011;56:98–105.
17. Nakano N, Hangai M, Nakanishi H, Mori S, Nukada M, Kotera Y, Ikeda HO, Nakamura H, Nonaka A, Yoshimura N. Macular ganglion cell layer imaging in preperimetric glaucoma with speckle noise-reduced spectral domain optical coherence tomography. *Ophthalmology.* 2011;118:2414–26.
18. Yamada H, Hangai M, Nakano N, Takayama K, Kimura Y, Miyake M, Akagi T, Ikeda HO, Noma H, Yoshimura N. Asymmetry analysis of macular inner retinal layers for glaucoma diagnosis. *Am J Ophthalmol.* 2014;158:1318–29.